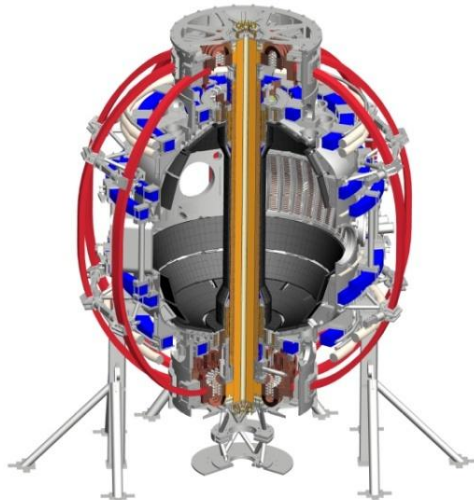


NSTX-U Research Highlights and Plans

Jonathan Menard, PPPL
For the NSTX Research Team

Coll of Wm & Mary
 Columbia U
 CompX
 General Atomics
 FIU
 INL
 Johns Hopkins U
 LANL
 LLNL
 Lodestar
 MIT
 Lehigh U
 Nova Photonics
 ORNL
 PPPL
 Princeton U
 Purdue U
 SNL
 Think Tank, Inc.
 UC Davis
 UC Irvine
 UCLA
 UCSD
 U Colorado
 U Illinois
 U Maryland
 U Rochester
 U Tennessee
 U Tulsa
 U Washington
 U Wisconsin
 X Science LLC

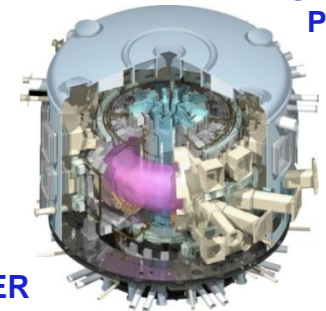
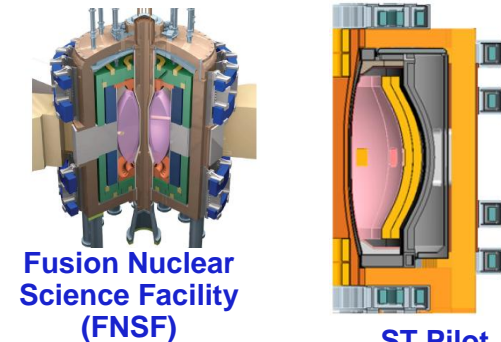
IAEA FEC Meeting
October 2012



Culham Sci Ctr
 York U
 Chubu U
 Fukui U
 Hiroshima U
 Hyogo U
 Kyoto U
 Kyushu U
 Kyushu Tokai U
 NIFS
 Niigata U
 U Tokyo
 JAEA
 Inst for Nucl Res, Kiev
 Ioffe Inst
 TRINITY
 Chonbuk Natl U
 NFRI
 KAIST
 POSTECH
 Seoul Natl U
 ASIPP
 CIEMAT
 FOM Inst DIFFER
 ENEA, Frascati
 CEA, Cadarache
 IPP, Jülich
 IPP, Garching
 ASCR, Czech Rep

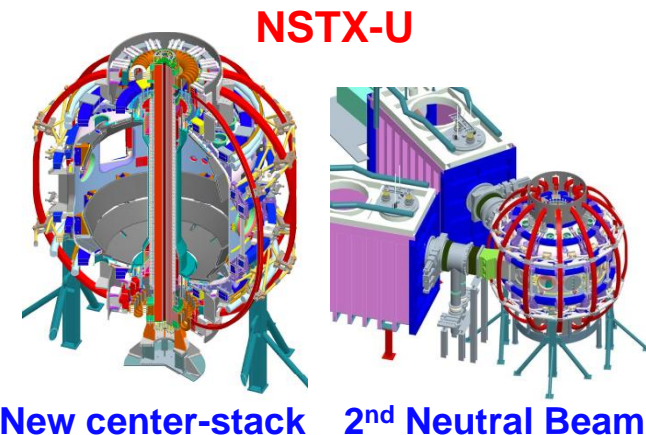
NSTX research targets predictive physics understanding needed for fusion energy development facilities

- Enable key ST applications
 - Move toward steady-state ST FNSF, pilot plant
 - Close key gaps to DEMO
- Extend understanding to tokamak / ITER
 - Leverage ST to develop predictive capability



Present Research

- Develop key physics understanding to be tested in unexplored, hotter ST plasmas
 - Study high beta plasma transport and stability at **reduced collisionality, extended pulse**
 - Prototype methods to mitigate **very high heat/particle flux**
 - Move toward **fully non-inductive operation**

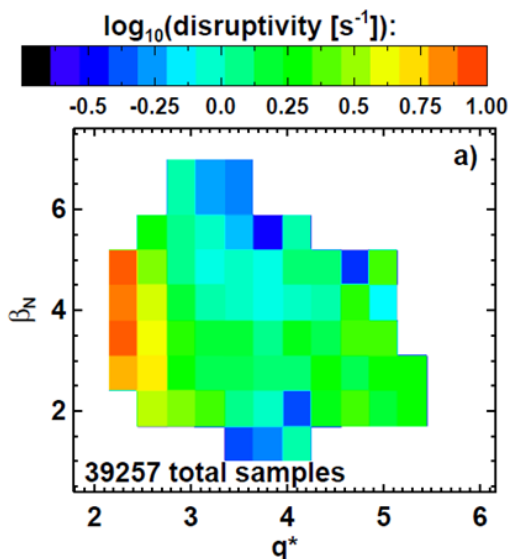


Disruption detection & warning analysis of NSTX being developed for disruption avoidance in NSTX-U, potential application to ITER

Disruptivity

- All discharges since 2005 with 1/3 ms sampling time

- Recorded equilibrium and kinetic parameters, disruption statistics



- Physics results

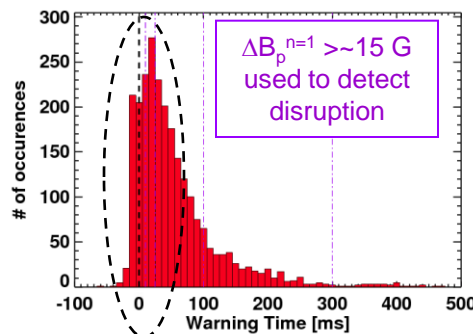
- Minimal disruptivity at relatively high $\beta_N \sim 6$; $\beta_N / \beta_N^{\text{no-wall}(n=1)} \sim 1.3\text{-}1.5$
 - Consistent with specific disruption control experiments
- Strong disruptivity increase for $q^* < 2.5$
- Strong disruptivity increases for lowest rotation

Gerhardt EX/9-3

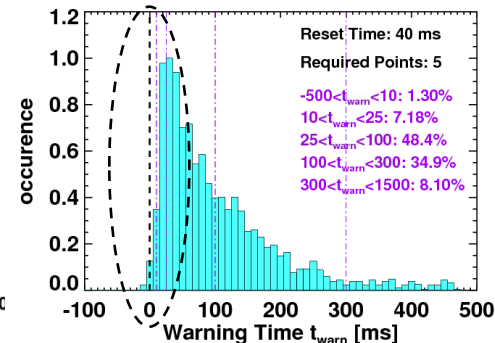
Warning Algorithms

- Disruption warning algorithm shows high probability of success
 - Based on combinations of threshold based tests; no machine learning

Statistics for a single threshold test



Statistics of full warning algorithm

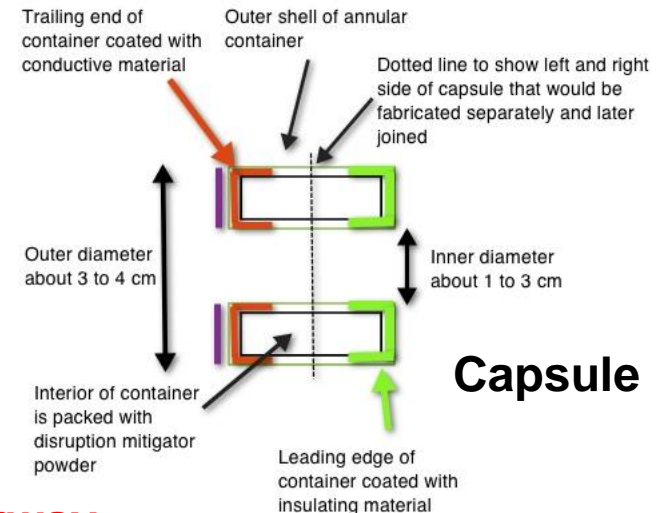
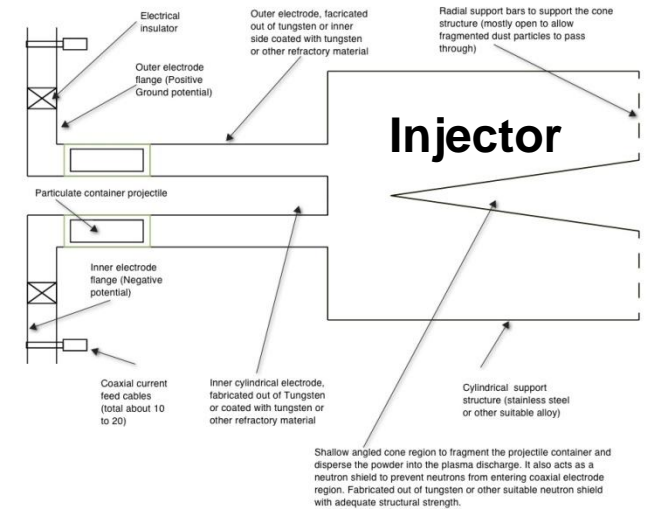


- Results & Physics implications

- $\sim 98\%$ disruptions flagged with at least 10ms warning, $\sim 6\%$ false positives
- Most false positives are due to “near disruptive” events
 - Early MHD slows ω_ϕ
 - recoverable Z motion

Exploring electromagnetic massive particle delivery system with potential advantages over conventional methods for disruption mitigation in ITER

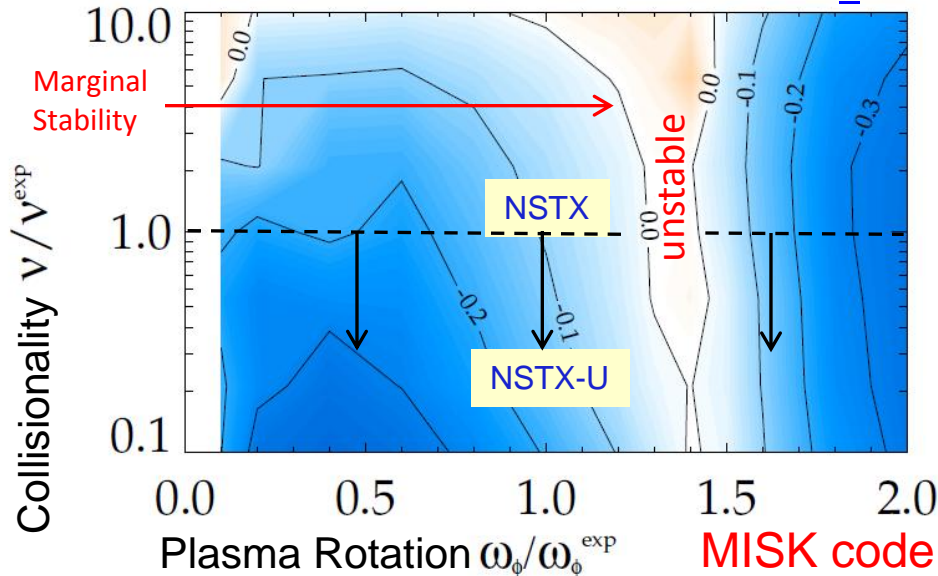
- Well suited for long stand-by mode operation:
 - Large particle inventory
 - All particles delivered at nearly the same time
 - Particles tailored to contain multiple elements in different fractions and sizes
 - Single system for varying initial plasma parameters
 - Tailored particles fully ionized only in higher current discharges
 - Particle penetration not impeded by B-fields
- Toroidal nature and conical disperser ensures that:
 - The capsule does not enter the tokamak intact
 - The capsule will fragment symmetrically and deliver a uniform distribution of particles (or via. tapered final section)
- Coaxial Rail Gun is a fully electromagnetic system with no moving parts, so should have high reliability from long stand-by mode to operate on demand:
 - Conventional gas guns will inject gas before capsule
- **Detailed design of a proto-type system now underway**



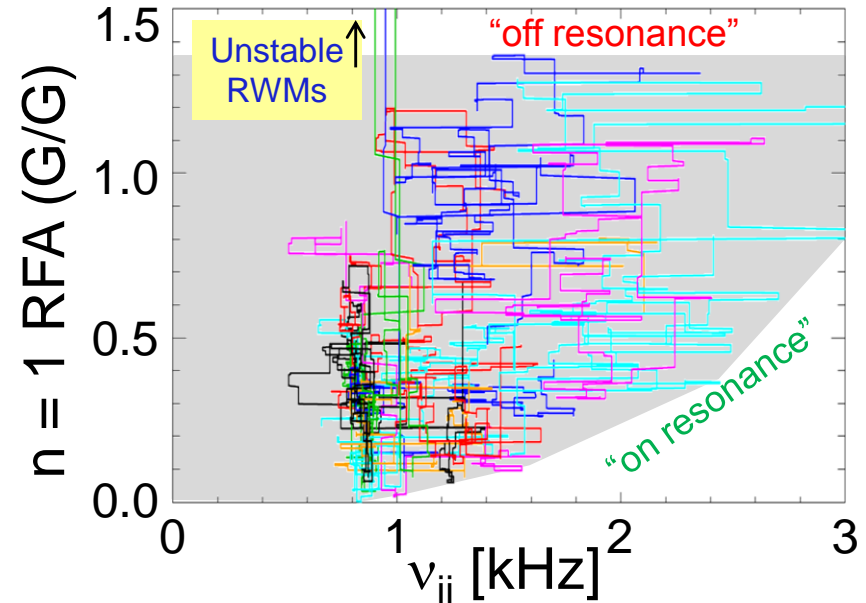
R. Raman et al, U. Washington

Measurements of global stability vs. collisionality support kinetic RWM stability theory, provide guidance for NSTX-U, ITER-AT

Theory: RWM growth rate contours ($\gamma\tau_{w\perp}$)



Exp: Resonant Field Amplification (RFA) vs ν



- ❑ Two competing effects at lower ν
 - ❑ Collisional dissipation reduced
 - ❑ Stabilizing resonant kinetic effects enhanced (contrasts early theory)

Expectations at lower ν

- ❑ More stabilization near ω_ϕ resonances; almost no effect off-resonance

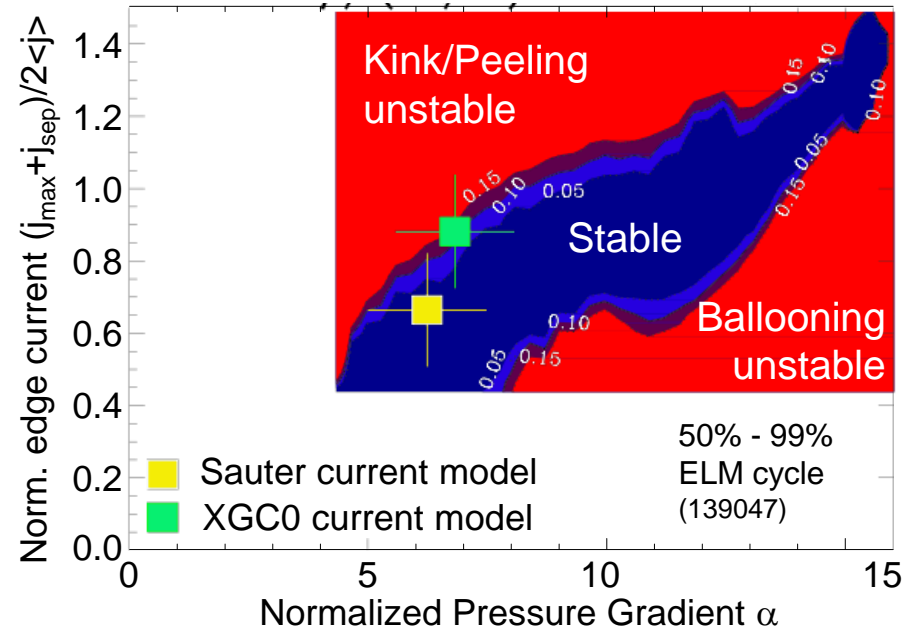
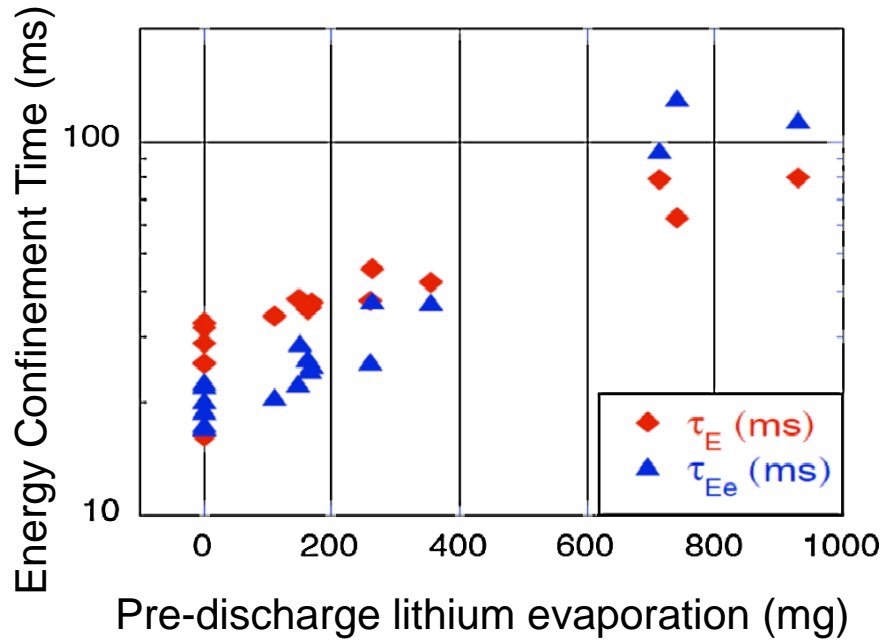
- ❑ Mode stability directly measured in experiment using MHD spectroscopy
 - ❑ Decreases with ν at lower RFA ("on resonance")
 - ❑ Independent of ν at higher RFA ("off resonance")

$$\text{RFA} = \frac{B_{\text{plasma}}}{B_{\text{applied}}}$$

Berkery EX/P8-07

J. Berkery et al., PRL 106, 075004 (2011)

Find plasma characteristics change nearly continuously with increasing Li evaporation; also testing ELM stability theory



- ❑ Global parameters generally improve
- ❑ ELM frequency declines - to zero
 - ❑ ELMs stabilize
- ❑ Edge transport declines
 - ❑ As lithium evaporation increases, transport barrier widens, pedestal-top χ_e reduced

- ELMing plasmas reach kink/peeling limit
- Improved bootstrap current calculation in pedestal (XGC0) yields improved agreement with marginal stability

Maingi EX/11-2

Canik EX/11-2

Diallo EX/P4-04

Chang TH/P4-12

PPPL Lithium Granule Injector tested on EAST

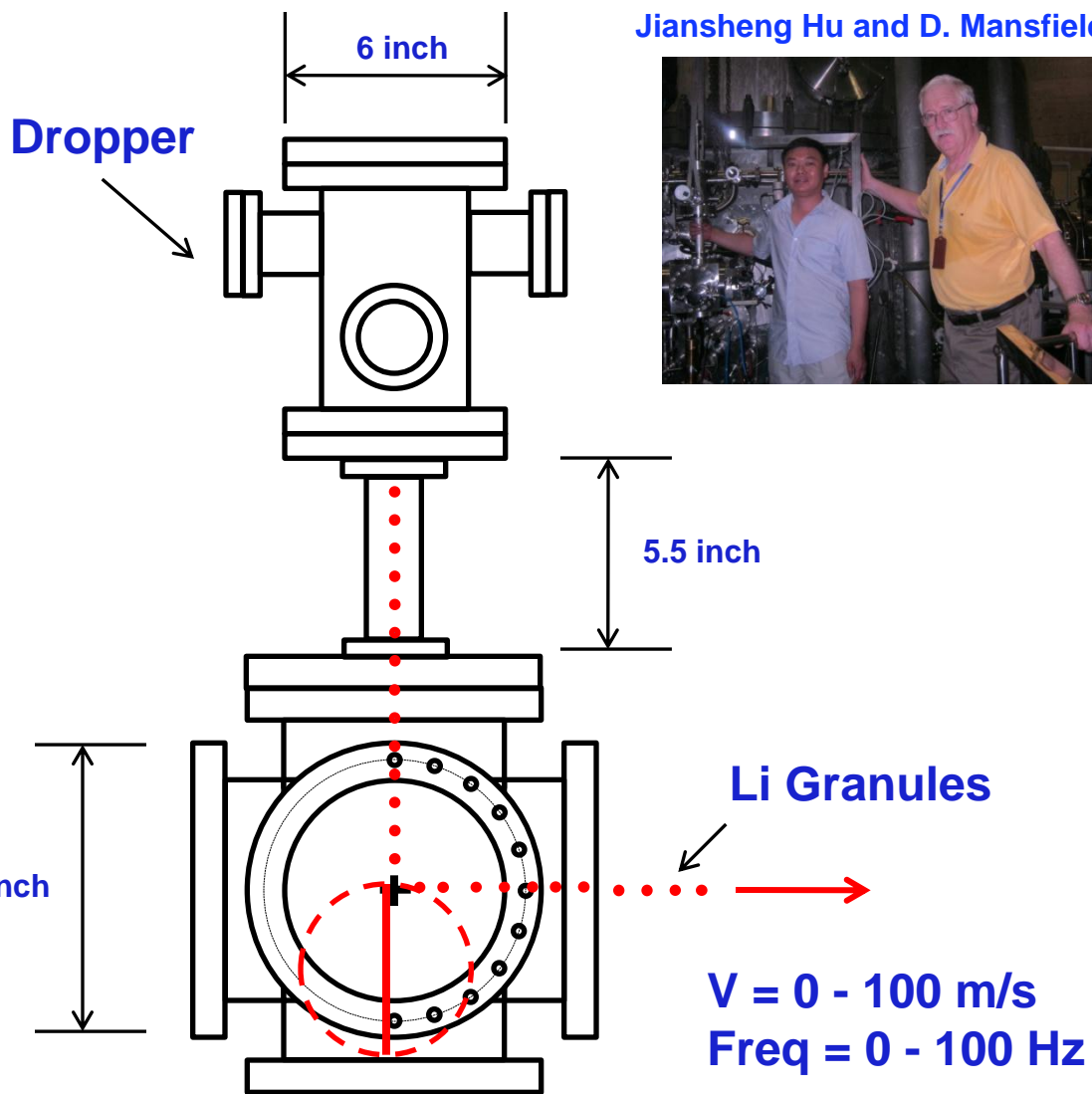
Dennis Mansfield (PPPL, retired)
Lane Roquemore (PPPL)

Independent Control:
Granule Size
(change between shots)

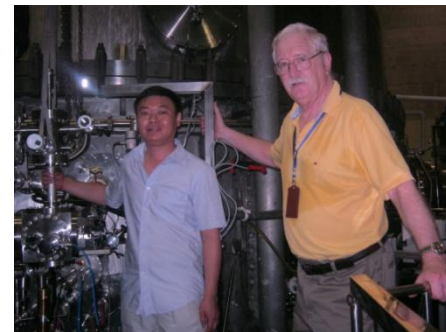


Injection Speed
(ramp during shots)

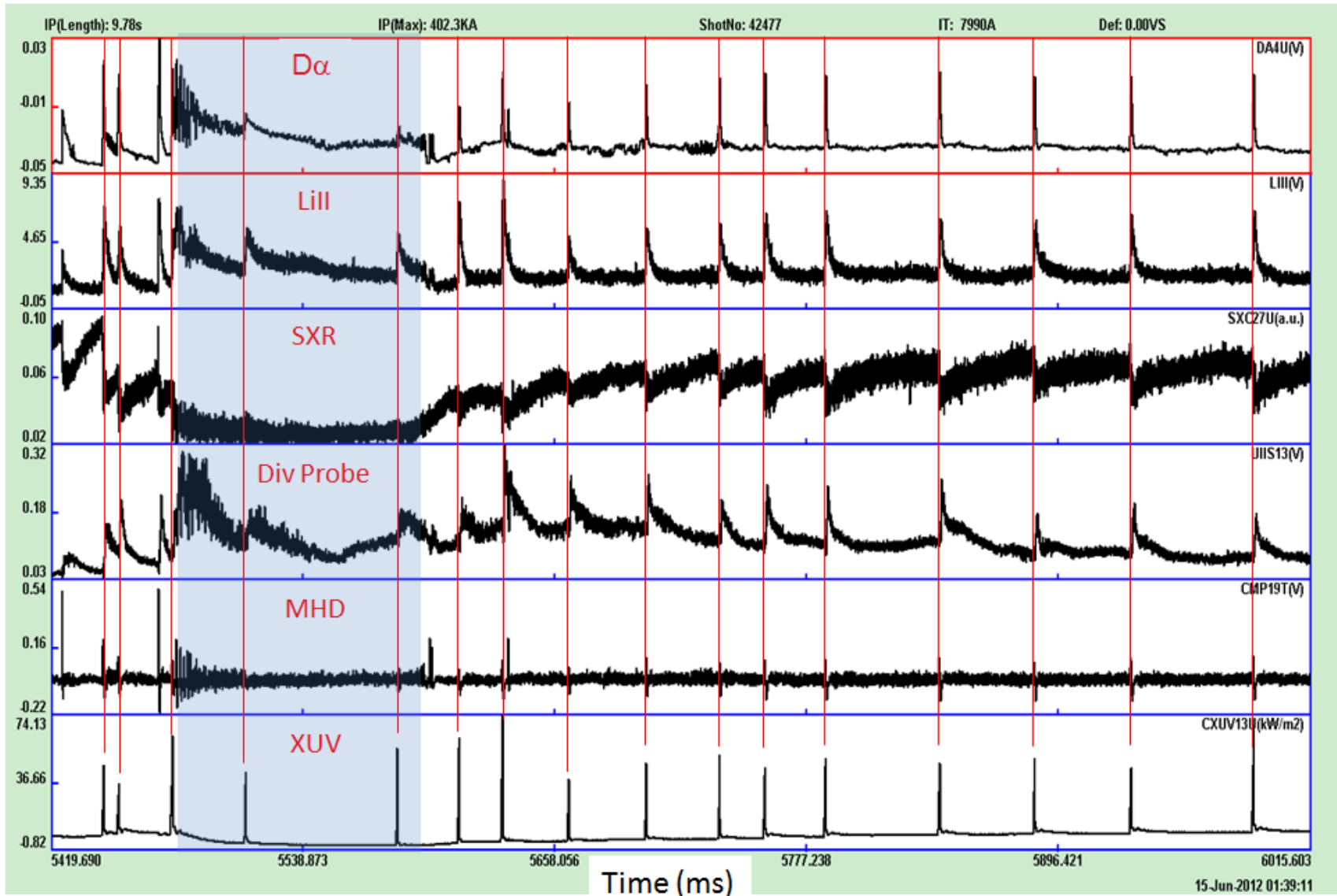
Pacing Frequency
(ramp during shots)



Jiansheng Hu and D. Mansfield

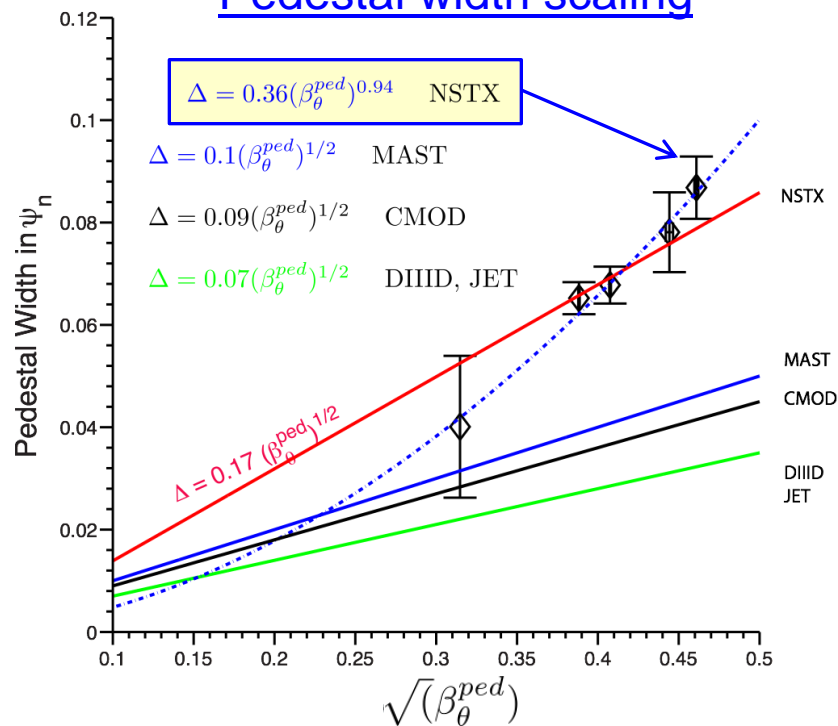


Triggered ~25Hz ELMs with 0.7mm Li granules at ~ 45 m/s → potentially very useful for triggering ELMs in Li-ELM free H-modes in NSTX-U, also ITER?



Pedestal width scaling similar to other experiments, but width is larger; turbulence correlation lengths consistent with theory

Pedestal width scaling



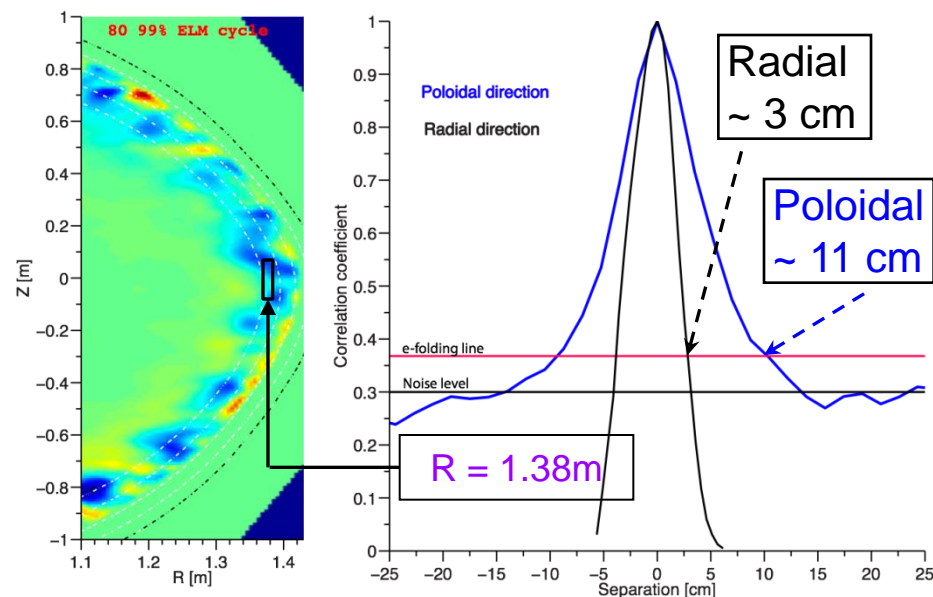
- ▣ Pedestal width scaling β_θ^α applies to multiple machines
- ▣ In NSTX, observed ped. width is larger
 - ▣ 1.7 x MAST, 2.4 x DIII-D
 - ▣ Data indicates stronger for NSTX: $\beta_\theta^{0.94}$ vs. $\beta_\theta^{0.5}$

Diallo EX/P4-04

A. Diallo, C.S. Chang, S. Ku (PPPL), D. Smith (UW), S. Kubota (UCLA)

Turbulence correlation lengths

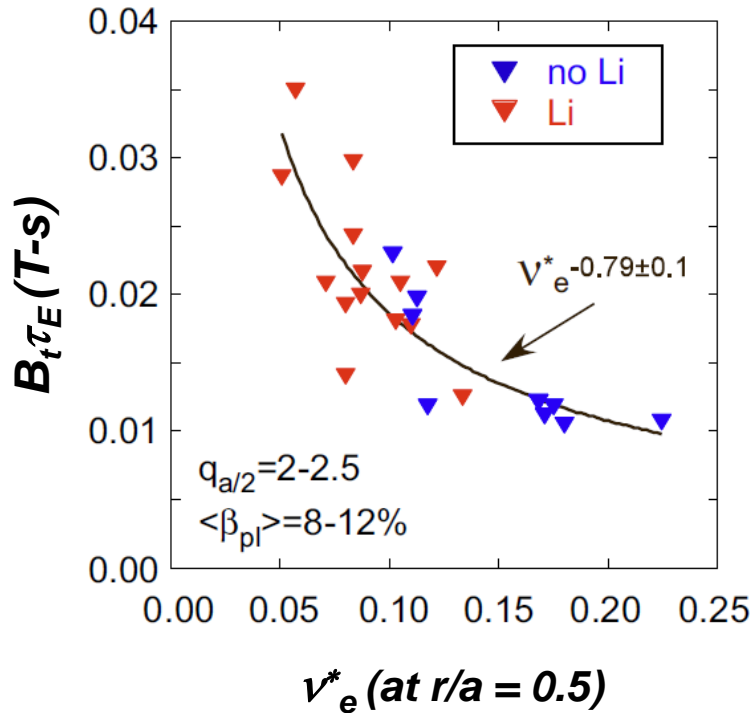
Theory: non-linear XGC1, Expt: BES



- ▣ Measured correlation lengths are consistent with theory
 - ▣ Radial (reflectometry) $\sim 2 - 4$ cm
 - ▣ Poloidal (BES) $\sim 10 - 14$ cm
 - spatial structure exhibits ion-scale microturbulence ($k_\theta \rho_i^{ped} \sim 0.1 - 0.2$)

Nonlinear microtearing simulations for NSTX consistent with measured electron heat transport dependence on collisionality

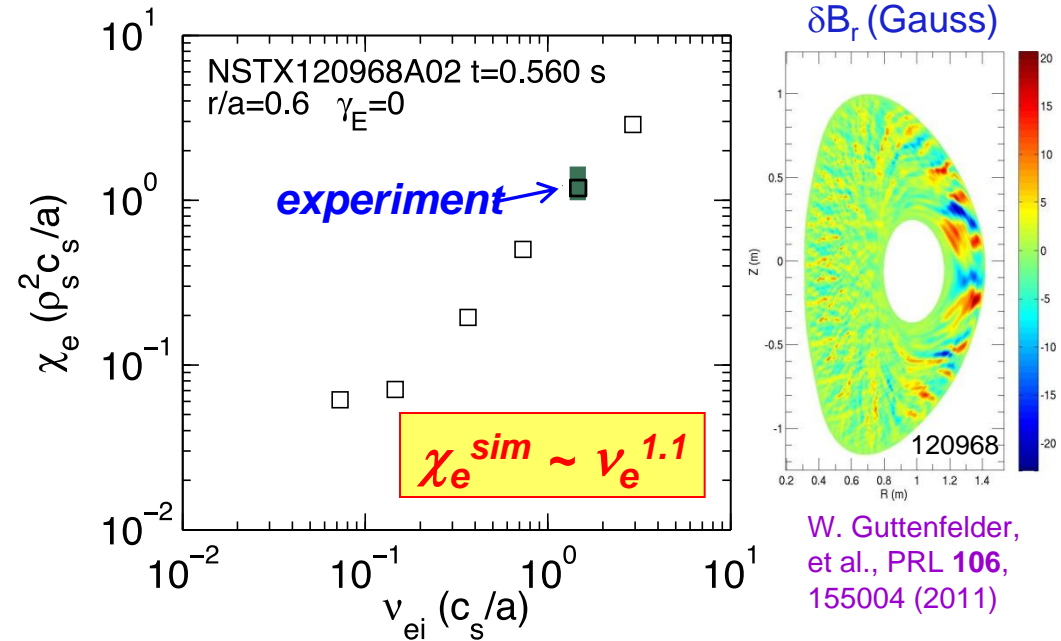
Experiment



- Increase in τ_E as v_e^* decreases
- Trend continues when lithium is used

Kaye EX/7-1

Theory

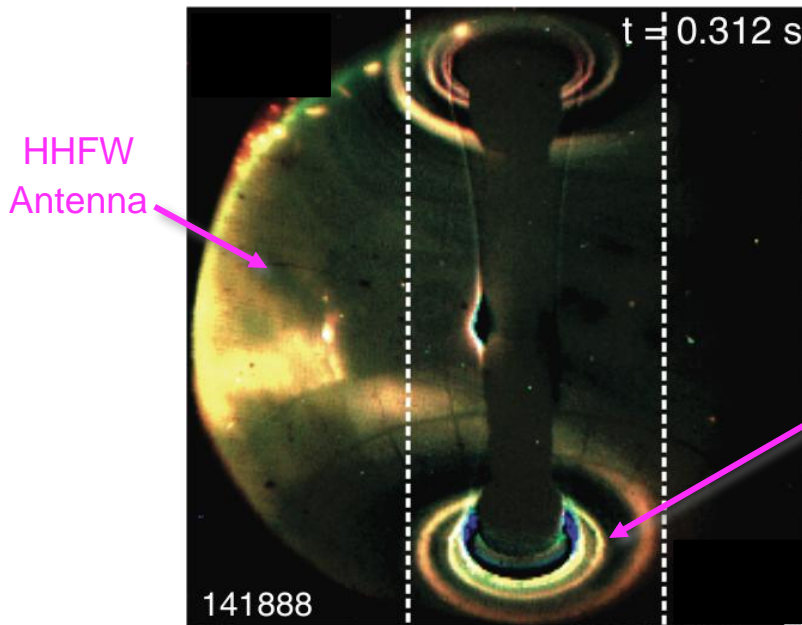


- Predicted χ_e and scaling $\sim v_e^{1.1}$ consistent with experiment ($\Omega \tau_E \sim B_t \tau_E \sim v_e^{*-0.8}$)
- Transport dominated by magnetic “flutter”
 - $\delta B_r / B \sim 0.1\%$ - possibly detectable by planned UCLA polarimetry system

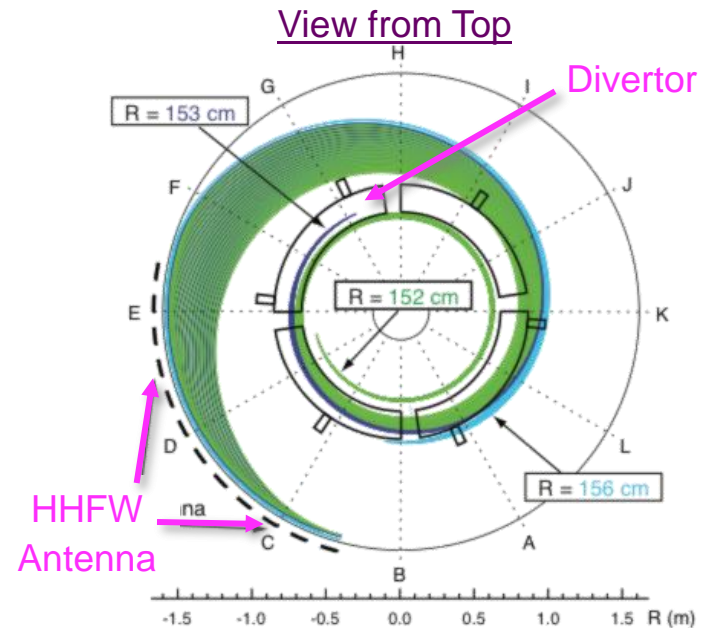
Guttenfelder TH/6-1

- NSTX-U computed to extend studies down to $< 1/4$ of present v_e^*

Significant fraction of the NSTX HHFW power may be lost in the SOL in front of antenna and flow to the divertor region



Visible camera image shows edge RF power flow follows magnetic field from antenna to divertor



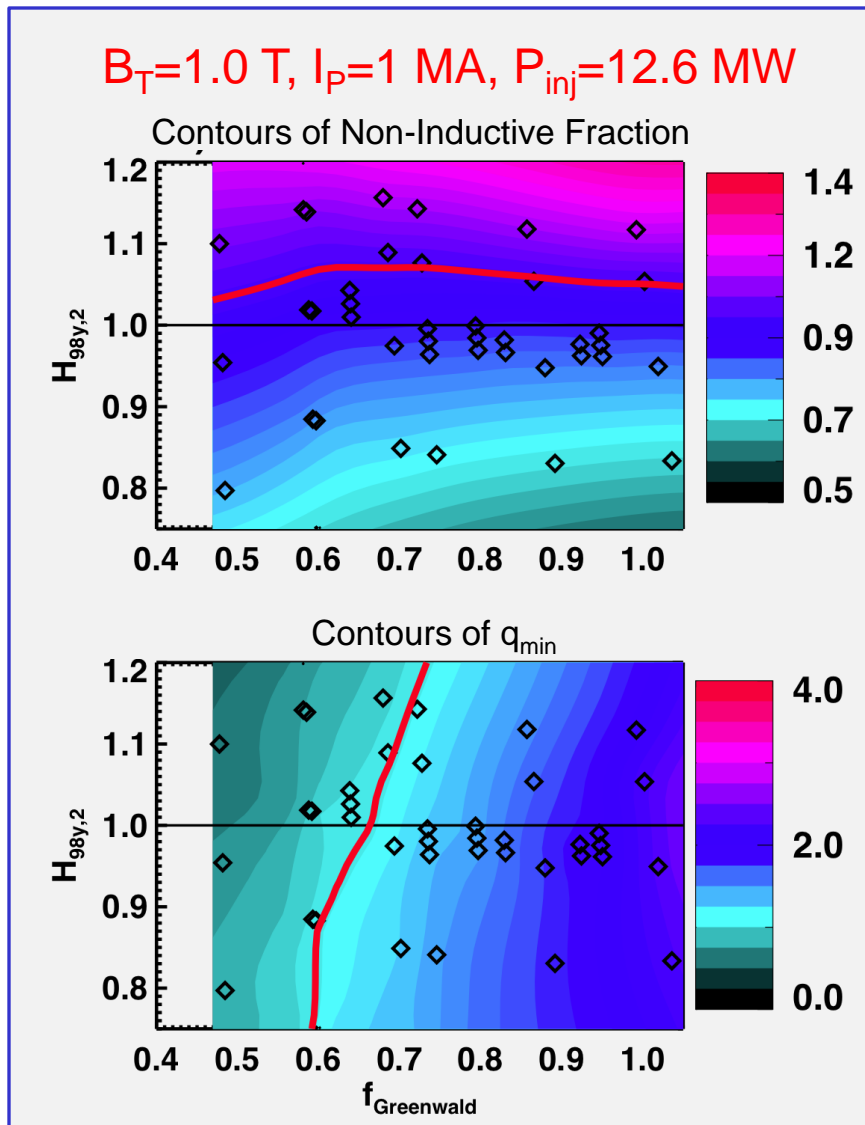
SPIRAL results show field lines (green) spiraling from SOL in front of HHFW antenna to divertor

R. J. Perkins, *et al.*, PRL (2012)

Perkins EX/P5-40

- Field line mapping predicts RF power deposited in SOL, not at antenna face
 - 3D AORSA will assess surface wave excitation in NSTX-U
- NSTX-U experiments and modeling to emphasize HHFW heating of high NBI power, long-pulse H-modes → assess effect of varying outer gap

100% non-inductive NSTX-U operating points projected for range of toroidal fields, densities, and confinement levels



Projected Non-Inductive Current Levels for $\kappa \sim 2.85$, $A \sim 1.75$, $f_{GW} = 0.7$

B_T [T]	P_{inj} [MW]	I_P [MA]
0.75	6.8	0.6-0.8
0.75	8.4	0.7-0.85
1.0	10.2	0.8-1.2
1.0	12.6	0.9-1.3
1.0	15.6	1.0-1.5

- From GTS (ITG) and GTC-Neo (neoclassical):
 - $\chi_{i,ITG}/\chi_{i,Neo} \sim 10^{-2}$
 - Assumption of neoclassical ion thermal transport should be valid

NSTX-U team continuing to strongly support ITER through participation in ITPA joint experiments and activities

• Advanced Scenarios and Control (4)

- IOS-1.2 Study seeding effects on ITER baseline discharges
- IOS-4.1 Access conditions for advanced inductive scenario with ITER-relevant conditions
- IOS-4.3 Collisionality scaling of confinement in advanced inductive plasmas
- IOS-5.2 Maintaining ICRH coupling in expected ITER regime

• Boundary Physics (10)

- PEP-6 Pedestal structure and ELM stability in DN
- PEP-19 Edge transport under the influence of resonant magnetic perturbations
- PEP-23 Quantification of the requirements of ELM suppression by magnetic perturbations from internal off mid-plane coils
- PEP-25 Inter-machine comparison of ELM control by magnetic field perturbations from mid-plane RMP coils
- PEP-26 Critical edge parameters for achieving L-H transitions
- PEP-27 Pedestal profile evolution following L-H/H-L transition
- PEP-28 Physics of H-mode access with different X-point height
- PEP-31 Pedestal structure and edge relaxation mechanisms in I-mode
- PEP-32 Access to and exit from H-mode with ELM mitigation at low input power above P_{LH}
- DSOL-24 Disruption heat loads

• Macroscopic Stability (5)

- MDC-2 Joint experiments on resistive wall mode physics
- MDC-4 Neoclassical tearing mode physics – aspect ratio comparison
- MDC-14 Rotation effects on neoclassical tearing modes
- MDC-15 Disruption database development
- MDC-17 Physics-based disruption avoidance

• Transport and Turbulence (7)

- TC-9 Scaling of intrinsic plasma rotation with no external momentum input
- TC-10 Experimental identification of ITG, TEM and ETG turbulence and comparison with codes
- TC-12 H-mode transport at low aspect ratio
- TC-14 RF rotation drive
- TC-15 Dependence of momentum and particle pinch on collisionality
- TC-17 ρ^* scaling of the intrinsic torque
- TC-19 Characteristics of I-mode plasmas

• Wave-Particle Interactions (4)

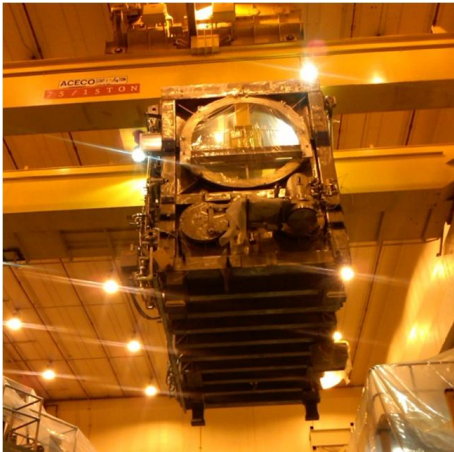
- EP-2 Fast ion losses and redistribution from localized AEs
- EP-3 Fast ion transport by small scale turbulence
- EP-4 Effect of dynamical friction (drag) at resonance on non-linear AE evolution
- EP-6 Fast ion losses and associated heat loads from edge perturbations (ELMS and RMPs)

NSTX typically actively participates in ~25 Joint Experiments/Activities

Rapid progress being made on NSTX Upgrade Project

First plasma anticipated mid-2014

Beam box craned over NSTX



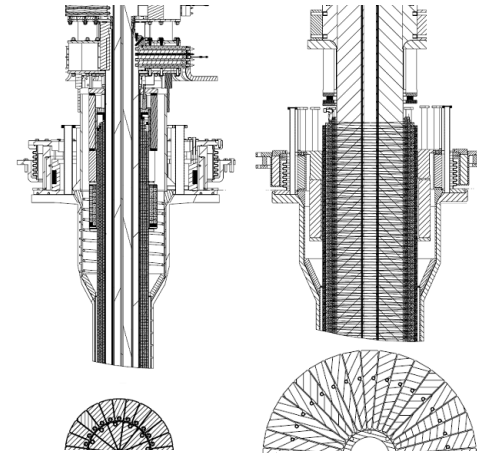
Box + cryo-panels next to NSTX



- 2nd NBI box moved into place
 - 1 month ahead of schedule

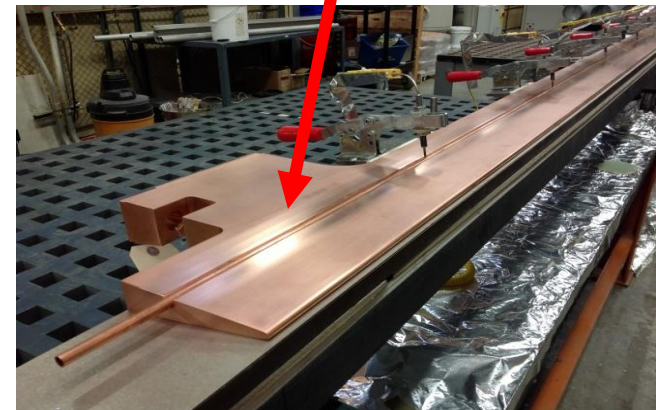
Old center stack

NEW Center Stack



TF OD = 20cm

TF OD = 40cm



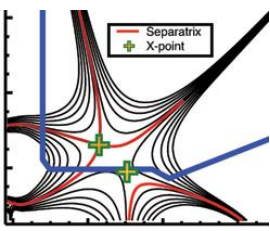
- Center-stack upgrade TF conductors being fabricated

Formulating FY2014-18 5 year plan to access new ST regimes with Upgrade + additional staged & prioritized upgrades

2009	2010	2011	2012	2013	2014	2015	2016	2017	2018
------	------	------	------	------	------	------	------	------	------

1 MA Plasma	Upgrade Outage	1.5 → 2 MA Plasma
-------------	----------------	-------------------

- CHI Control Coils
- LLD
- Moly-tile
- HHFW Upgrade

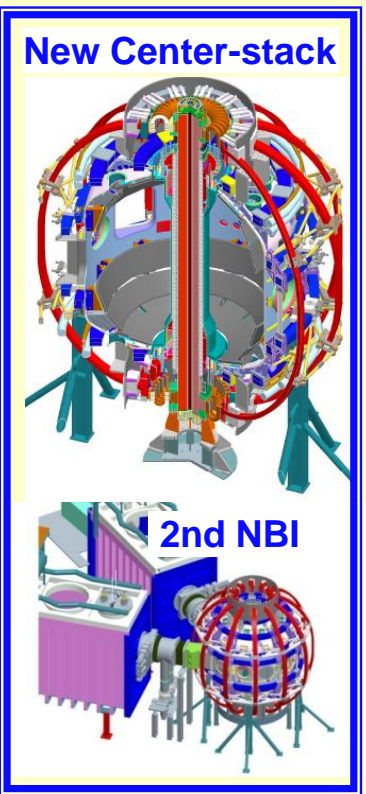


“Snowflake”



Lithium

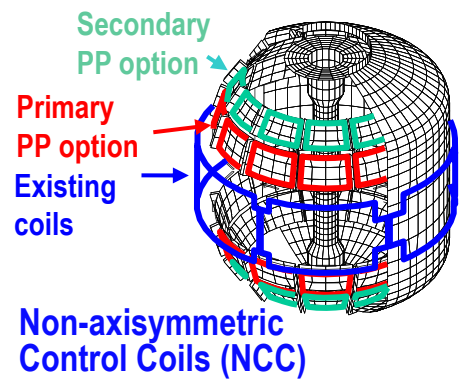
- New Center-Stack
- 2nd NBI



- 0.5 MA CHI
- ECH/EBW 1MW → 2 MW
- 1 MA CHI / Plasma Gun

- 0.5 MA Plasma Gun
- Long-pulse Divertor

- NCC Upgrade



NSTX Upgrade research goals in support of FNSF and ITER

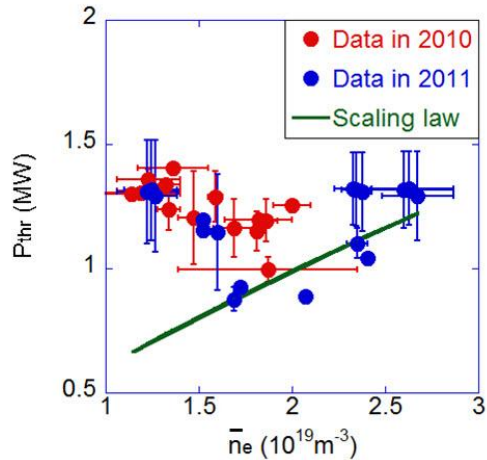
- Low collisionality plasma regimes
- 100% non-inductive operation
- Long-pulse, high power divertor
- Advanced high-β scenarios



NOTE: Upgrade operation would be delayed ~1 year to mid-2015 w/o incremental, other follow-on upgrades are further delayed

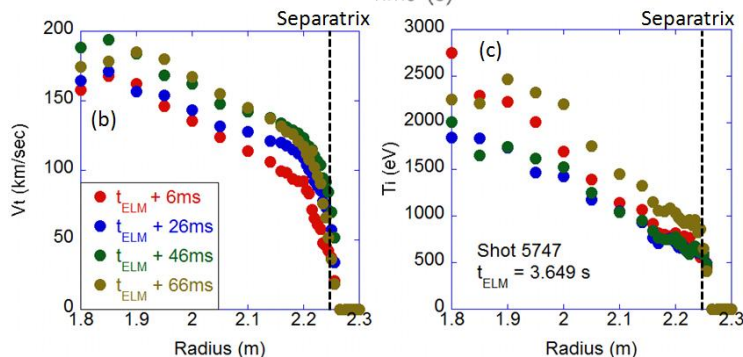
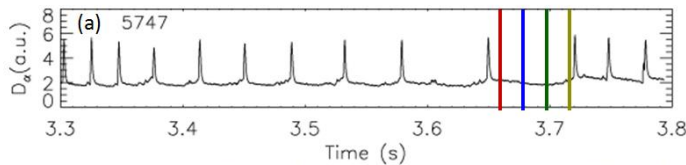
Collaboration Highlights

H-mode power threshold and confinement / ELM study at KSTAR



Measured L-H power threshold in low density regime¹

- Dependence of L-H power threshold (P_{thr}) on density revealed roll-over at $n_e \sim 2e19 \text{ m}^{-3}$, while there is no such a dependence in the present multi-machine scaling laws.
- Four types of ELMy H-mode were identified even with low NBI power ($P_{NBI} = 1.5\text{MW}$); (1) large type-I ELMs with $H_{98}=0.8-0.9$, (2) intermediate (possibly type-III) ELMs with $H_{98}=0.6-0.8$, (3) mixed (type-I + small) ELMs with $H_{98}=0.9-1.0$, and (4) small ELMs with $H_{98}=0.8-0.9$



V_t and T_i profile evolution during the ELM cycle¹

Profile measurement for type-I ELMy H-mode shows that the recovery of T_i pedestal after the ELM crash only occurs at the last stage of the inter-ELM period, *i.e.* $> 80\%$ of the ELM cycle. V_t and T_e pedestal continue to build up during the whole ELM cycle.

¹J-W. Ahn, ORNL submitted to NF (2012)

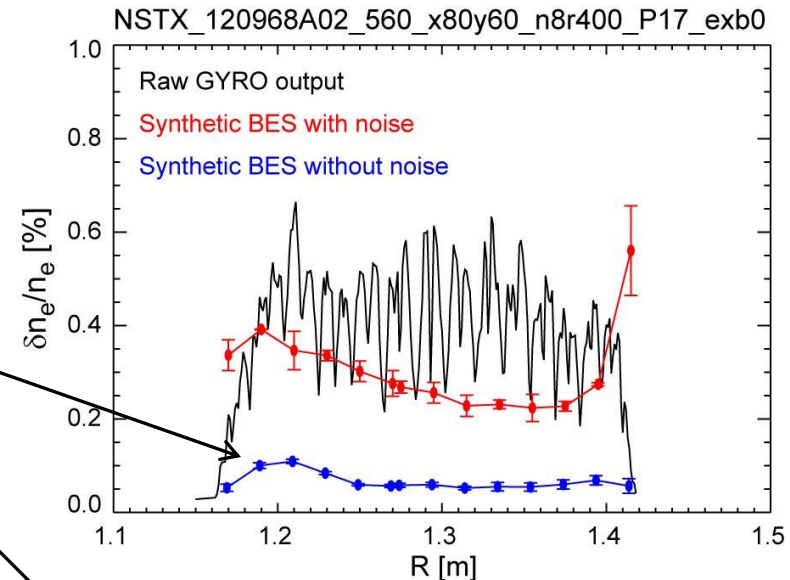
MAST-NSTX collaboration testing sensitivity of BES to microtearing turbulence through synthetic diagnostics

- Using nonlinear NSTX microtearing simulations from GYRO with synthetic diagnostic for MAST BES
 - Difficult to detect MT with expected signal-to-noise ratio (uncorrelated noise dominates)
 - If S/N can be increased (e.g. significant time averaging) MT features may be measurable, such as:
 - detectable correlated fluctuation levels ($\delta n/n \sim 0.1\%$)
 - large poloidal correlation lengths ($L_p \sim 15\text{-}20\text{ cm}$)

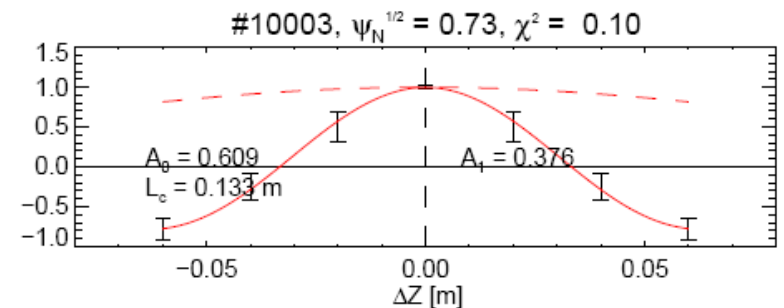
Future plans:

- Pursue non-linear simulations for MAST discharges with available BES data
- Propose experiments for FY13 at next MAST research forum (Dec 2012) to focus on relationship between collisionality scaling and microtearing turbulence

Density fluctuation (rms)



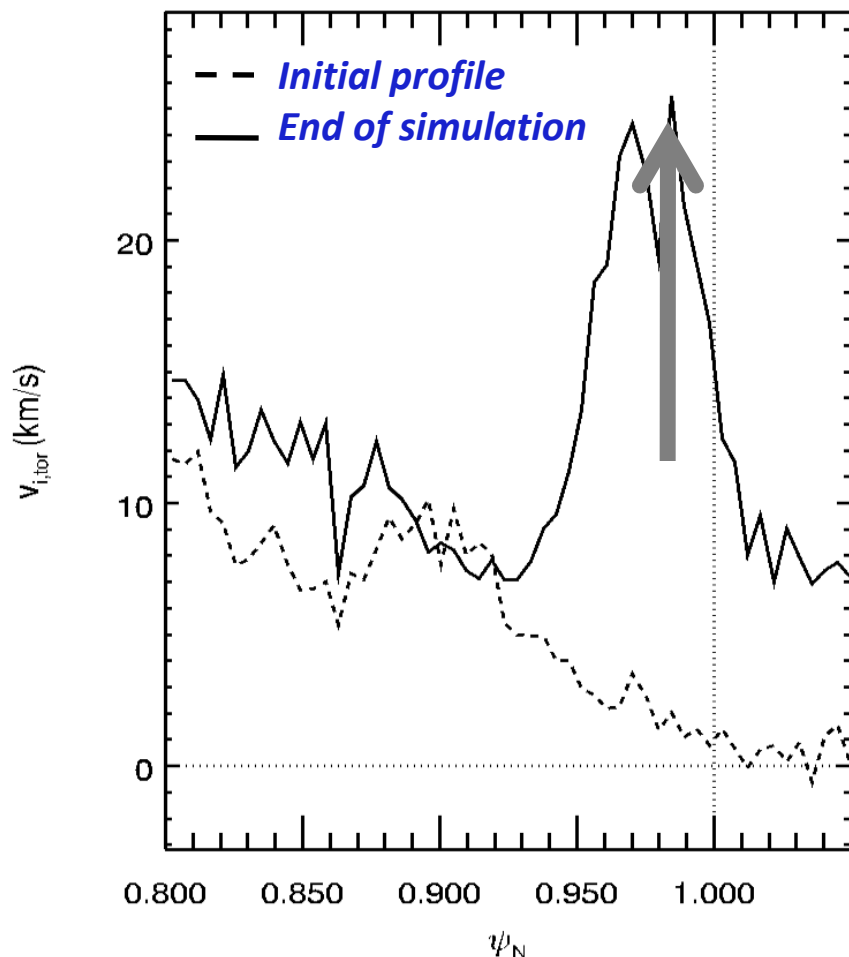
Poloidal correlation from synthetic diagnostic (without noise)



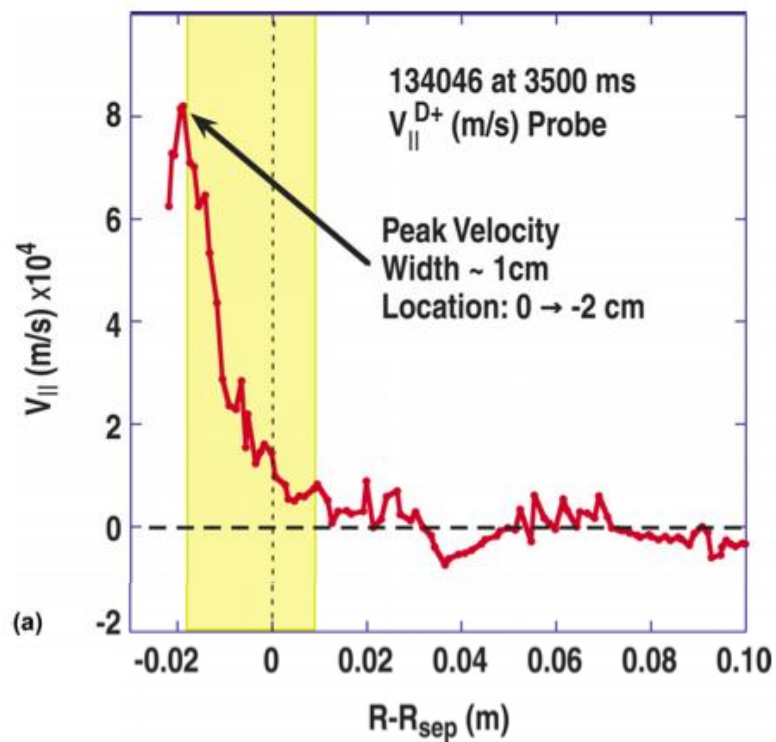
Kinetic neoclassical effects in DIII-D H-mode pedestal using XGC0

To help answer important questions on edge rotation, main-ion physics and SOL flows.

Preliminary results using XGC0 simulation of edge main-ion velocity driven by X-loss



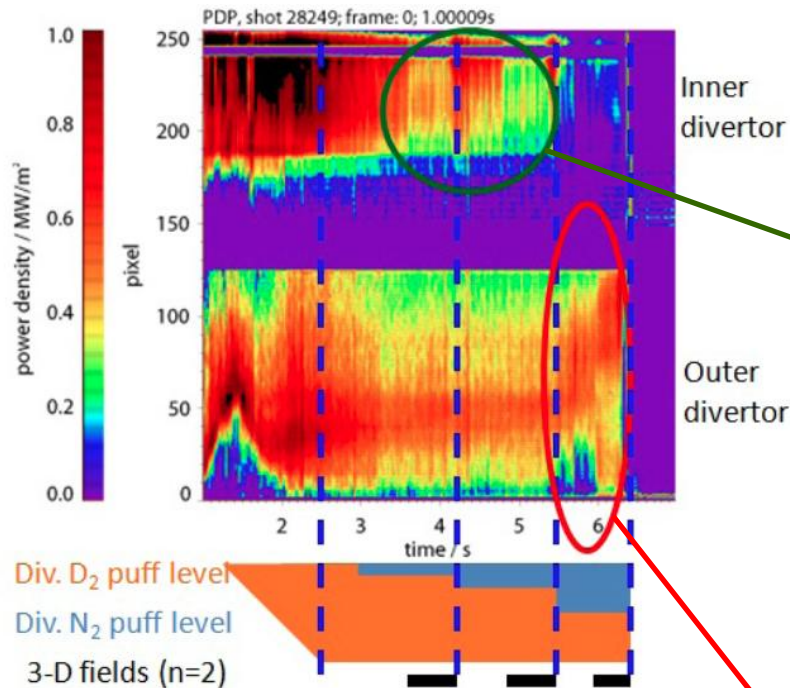
Deuterium edge velocity measured by Mach Probe
J.A. Boedo et al., PoP 18 032510 (2011)



D. Battaglia et al., (PPPL)

3-D Field Effects on Divertor Detachment Explored in ASDEX-U

Temporal evolution of divertor heat flux profile during the divertor gas puff and 3-D field application



- Deuterium gas puffing induced power detachment at outer divertor but particle detachment was only produced by additional nitrogen puffing
- 3-D fields ($n=2$) application reduced the inner divertor power density but there was no change at the outer divertor.
- Applied 3-D fields reduced particle detachment at the outer divertor, which is consistent with the NSTX result.

3-D fields brought the outer divertor heat zone back in, closer to the strike point (sign of power re-attachment, **similar to the observation in NSTX**) although the particle detachment was becoming stronger. This data suggests that there is a possibility of a de-coupling of the power and particle detachments.

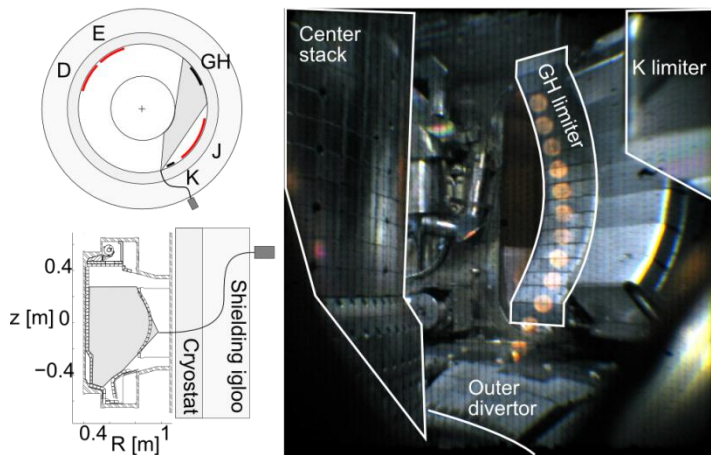
J-W. Ahn et al. ORNL

Material erosion studies at C-Mod

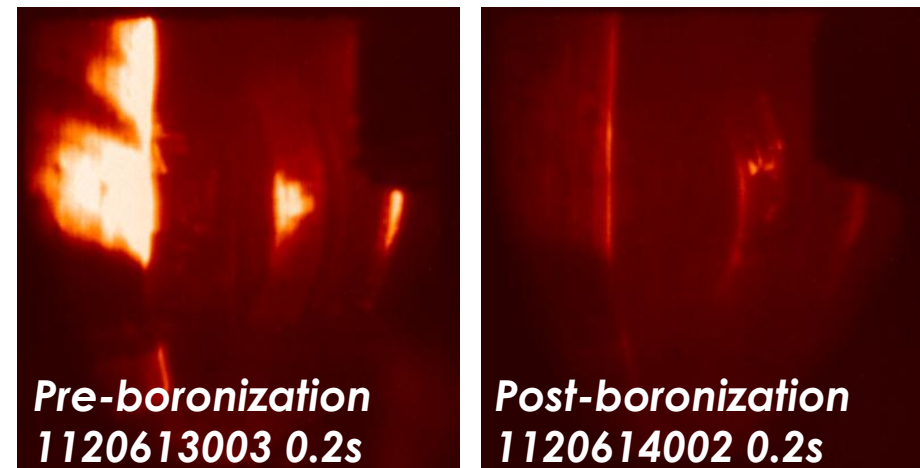
(high-Z wall and low-Z coatings)

- LLNL postdoc on-site at Alcator C-Mod tokamak
- Novel LLNL intensified camera diagnostic for molybdenum and boron erosion studies
 - Camera installed and calibrated, contributing to physics operations
 - Improving techniques for accounting for continuum and Plank emissions
 - Analyzing moly and boron limiter erosion and core moly penetration factors including RF, inner-wall startup, and boronization effects
- Collaboration with ADAS consortium on improved Mo I and Mo II atomic physics calculations for gross and net erosion measurements

Vlad Soukhanovskii et al., LLNL



LLNL moly camera viewing geometry

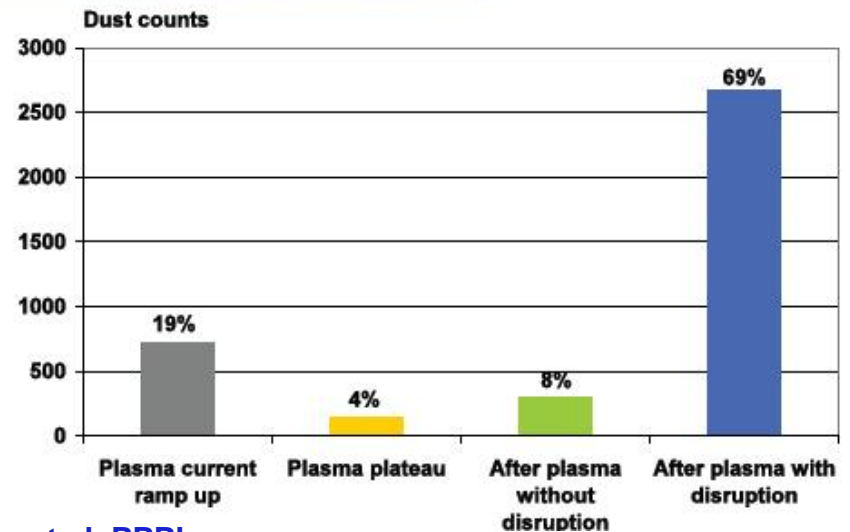
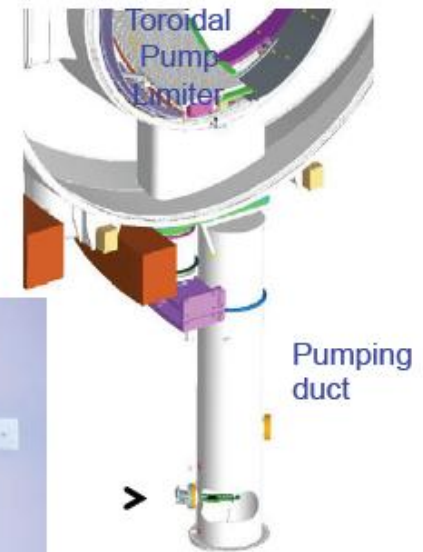
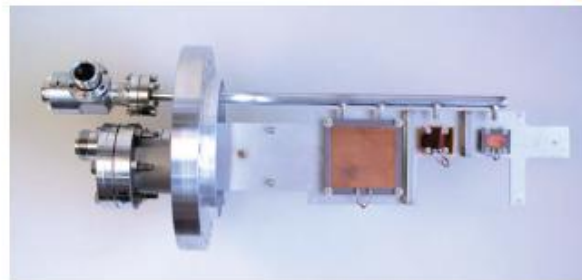


Mo I emission pre- and post-boronization in C-Mod

NSTX Dust Detector Demonstrated on Tore Supra

- Real-time dust measurement is necessary to safely manage dust in tokamak fusion reactors.
- A novel electrostatic dust detector was developed at PPPL and demonstrated on NSTX
see: 'First real-time detection of surface dust in a tokamak' C. H. Skinner et al., Rev. Sci. Instrum., 81 (2010) 10E102.
- Dust detection technology was successfully transferred to Tore Supra and used to correlate dust production with plasma events.
- 82% of the dust particles detected were due to disruptions
(including 13% detected during plasma current ramp up, following a shot with disruption).
For complete results see 'First results from dust detection during plasma discharges on Tore Supra' H. Roche et al., Phys. Scr. T145 (2011) 014022.

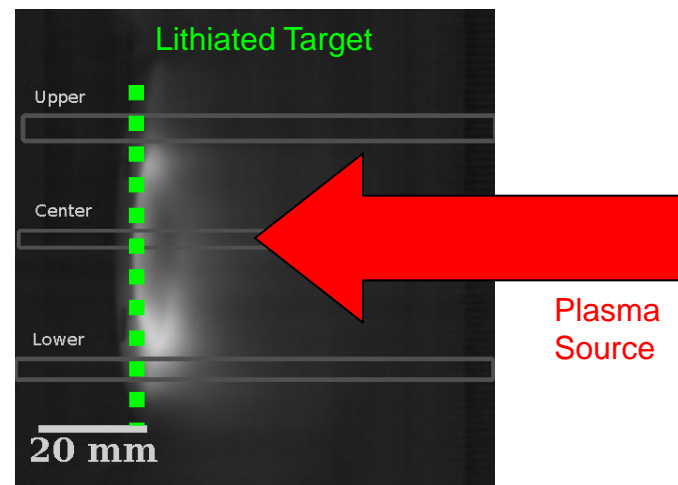
A set of 3 electrostatic detectors from PPPL



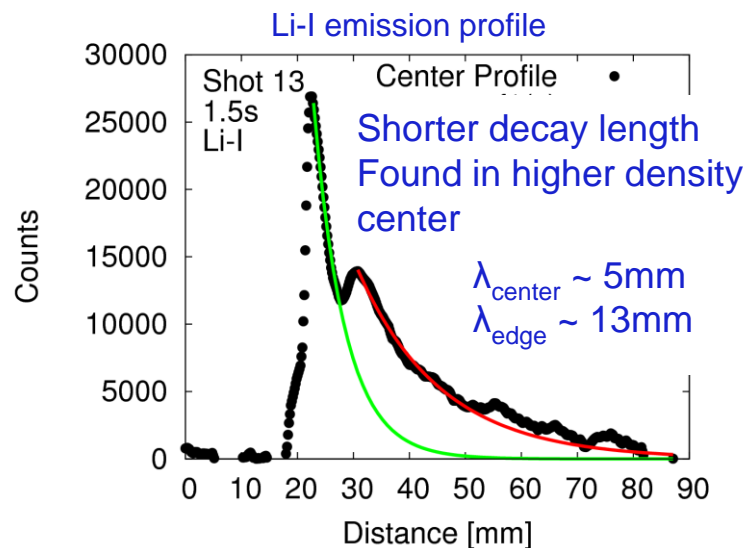
C. Skinner et al, PPPL

Lithium transport near divertor target being studied with Magnum-PSI linear test stand

- Transport of eroded lithium needed for plasma modeling and PFC development
 - Heat flux reduction via lithium radiation in the SOL – how does it get there?
 - Control of lithium inventory critical to reactors to avoid tritium codeposition and build-up
- Magnum-PSI reproduces divertor plasmas on target
 - Lithiated TZM example shown
 - Emission profiles in known background plasma provide basis for testing transport models



Li-I emission during exposure



M. Jaworski et al, PPPL